

Password-conditioned Anonymization and Deanonimization with Face Identity Transformers

Xiuye Gu^{1,4}, Weixin Luo^{2,4}, Michael S. Ryoo³, and Yong Jae Lee⁴

¹Stanford University

²ShanghaiTech University

³Stony Brook University

⁴UC Davis

Abstract

Cameras are prevalent in our daily lives, and enable many useful systems built upon computer vision technologies such as smart cameras and home robots for service applications. However, there is also an increasing societal concern as the captured images/videos may contain privacy-sensitive information (e.g., face identity). We propose a novel face identity transformer which enables automated photo-realistic password-based anonymization as well as deanonymization of human faces appearing in visual data. Our face identity transformer is trained to (1) remove face identity information after anonymization, (2) make the recovery of the original face possible when given the correct password, and (3) return a wrong—but photo-realistic—face given a wrong password. Extensive experiments show that our approach enables multimodal password-conditioned face anonymizations and deanonymizations, without sacrificing privacy compared to existing anonymization approaches.

1. Introduction

As computer vision technology is becoming more integrated into our daily lives, addressing privacy and security questions is becoming more important than ever. For example, smart cameras and robots in homes are being used for service applications, but their recorded videos often contain sensitive information of their users. In the worst case, a hacker could intrude these devices and gain access to private information.

Recent anonymization techniques aim to alleviate such privacy concerns by redacting privacy-sensitive data like face identity information. Some methods [3, 26] perform low-level image processing such as extreme downsampling, image masking, etc. A recent paper proposes to *learn* a face anonymizer that modifies the identity of a face while preserving activity relevant information [23]. However,

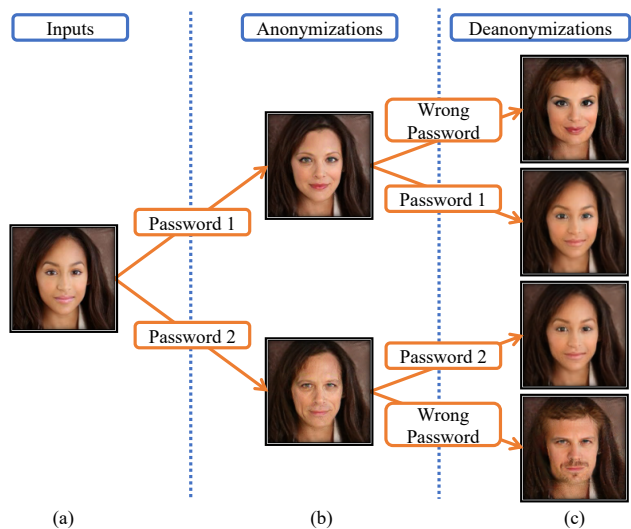


Figure 1: Our system never stores users’ faces (a) on disk, and instead only stores the anonymized faces (b). When a user provides a correct recovery password, s/he will get the deanonymized face back (c). If a hacker invading their privacy inputs a wrong password, s/he will get a face whose identity is different from the original as well as the anonymized face (c). The photo-realism of the modified faces is meant to fool the hacker by providing no clues as to whether the real face was recovered.

none of these existing techniques consider the fact that the video/image owner (and his/her friends, family, etc.) may want to see the *original* identities but not the anonymized ones. For example, people may not want their real faces to be saved directly on home security cameras due to privacy concerns; however, remote family members may want to see the real faces from time to time.

This problem poses an interesting tradeoff between privacy and accessibility. On the one hand, we would like a system that can anonymize sensitive regions (face identity) so that even if a hacker were to gain access to such data,

they would not be able to know who the person is (without additional identity revealing meta-data). On the other hand, the owner of the visual data inherently wants to see the original data, not the anonymized one.

This paper proposes to address this issue. Specifically, we introduce a *face identity transformer* that can both *anonymize and deanonymize (recover)* the original image, while maintaining privacy. Our main idea is the introduction of a password scheme, in which the anonymizations and deanonymizations are conditioned on passwords that control how the identity of a face should change. Specifically, given an original face, our face identity transformer outputs different anonymized face images with different passwords (Fig. 1b). Then, given an anonymized face, the original face is recovered only if the correct password is provided (Fig. 1c, ‘Password 1/2’). We further increase security as follows: Given an anonymized face, if a wrong password is provided, then the anonymized face changes to a new identity, which is still different from the original identity (Fig. 1c, ‘Wrong Password’). Moreover, each wrong password maps to a unique identity. In this way, we provide security via ambiguity: even if a hacker guesses the correct password, without having access to any other identity revealing meta-data, it is extremely difficult to know that they have guessed the correct password since each password—regardless of whether it is correct or not—always leads to a different realistic identity.

To enforce the face identity transformer to output different anonymized face identities with different passwords, we maximize the feature-level dissimilarity between pairs of anonymized faces that have different passwords. To enforce it to recover the original face with the correct password, we train it to anonymize and then recover the correct identity only when given the correct password and inverse-password pair, and to produce a new identity otherwise. Lastly, we maximize the feature dissimilarity between an anonymized face and its deanonymized face with a wrong password.

We note that our approach is related to cryptosystems like RSA [24]. The key difference is that cryptosystems do not produce encryptions that are visually recognizable to human eyes. However, in various scenarios, users may want to understand what is happening in anonymized visual data. For example, people may share photos/videos over public social media with anonymized faces, but only their real-life friends have the passwords and can see their real faces to protect identity information. Moreover, with photorealistic anonymizations, one can easily apply existing computer vision based recognition algorithms on the anonymized images, unlike other schemes (*e.g.*, homomorphic encryption) that require developing new ad-hoc recognition methods specific to nonphotorealistic modifications, in which accuracy may suffer.

In our approach, only the anonymized data is saved to

disk (*i.e.*, conceptually, the anonymization would happen at the hardware-level via an embedded chipset – the actual implementation of which is outside the scope of this work). The advantage of this concept is that the hacker could never have direct access to the original data. Finally, although there may be other identity-revealing information such as gait, clothing, background, etc., our work entirely focuses on improving privacy of face identity information, but would be complementary to systems that focus on those other aspects.

Our experiments on CASIA [31], LFW [11], and FFHQ [13] show that the proposed method enables multimodal face anonymization as well as recovery of original face images, without sacrificing privacy compared to existing advanced anonymization [23] and classical image processing techniques including masking, noising, and blurring, etc.

2. Related work

Privacy-preserving visual recognition. This is the problem of detecting humans, their actions, and objects without accessing user-sensitive information in images/videos. Some methods employ extreme low-resolution downsampling to hide sensitive details [30, 6, 26, 25] but suffer from lower recognition performance in downstream tasks. Recent work [23] proposes to learn a video anonymizer that performs pixel-level modifications to remove people’s identity while preserving motion and object information for activity detection. Unlike our approach, none of these existing work employ a password scheme to condition the anonymization, and also do not perform deanonymization to recover the original face. Moreover, even if we could brute-force train a deanonymizer for these methods, there is no way to provide wrong recoveries upon wrong passwords, as our approach does.

Security/cryptography research on privacy-preserving recognition is also related *e.g.*, [8, 9]. The key difference is that these methods encrypt data in a secure but visually-uninterpretable way, whereas our goal is to anonymize the data in a way that is still interpretable to humans. Differential privacy [1, 32] is also related but its focus is on protecting privacy in the training data whereas ours is on anonymizing visual data during the inference stage.

Face image manipulation and conditional GANs. Researchers have studied pixel-level synthesis and editing of realistic human faces [14, 19, 27, 13, 20, 2]. Conditional GANs generate data conditioned on an input signal (*e.g.*, edges, facial action units, text, latent code) [18, 21, 12, 33, 38, 20, 5, 28, 7, 22]. Our work builds upon these advances, but we differ significantly in our goal, which is to completely change the identity of a face (and also recover the original) for privacy-preserving visual recognition.

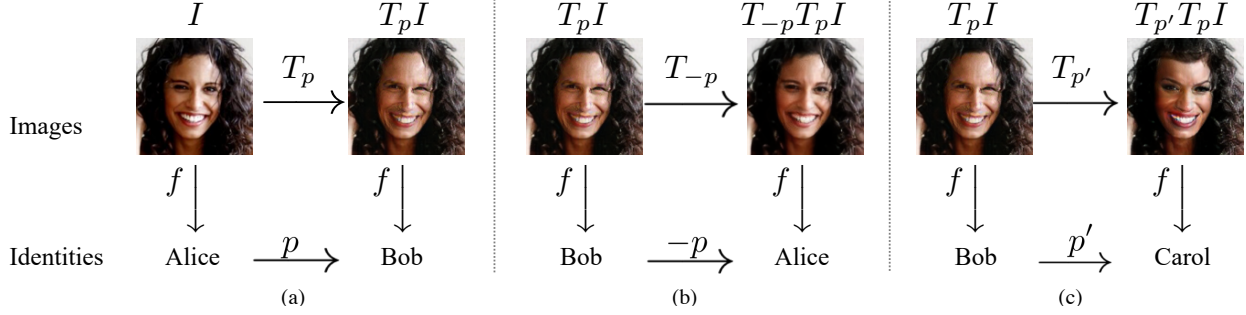


Figure 2: Privacy-preserving properties that our face identity transformer T learns. (a) Anonymization stage. (b) Deanonymization stage with correct recovery password. (c) Deanonymization stage with incorrect recovery password.

3. Desiderata

Our face identity transformer T takes as input a face image $I \in \Phi$ and a user-defined password $p \in P$, where Φ and P denote the face image domain and password domain. We use the notation $T_p I$ to denote the transformed image with input image I and password p . Before diving into the details, we first outline desired properties of a privacy-preserving face identity transformer.

Minimal memory consumption. Considering the limited memory space on most camera systems, a *single* face identity transformer that can both anonymize and deanonymize faces is desirable.

Photo-realism. We would like the transformer to maintain photo-realism for any transformed face image:

$$T_p I \in \Phi, \quad \forall p \in P, \forall I \in \Phi. \quad (1)$$

Photo-realism has three benefits: (1) a human who views the transformed images will still be able to interpret them; (2) one can easily apply existing computer vision algorithms on the transformed images; and (3) it's possible to confuse a hacker, since photo-realism cannot be used as a cue to differentiate the original face from an anonymized one.

Compatibility with background. The background B of the transformed face should be the same as the original:

$$B(T_p I) = B(I), \quad \forall p \in P, \forall I \in \Phi. \quad (2)$$

This will ensure that there are no artifacts between the face region and the rest of the image (*i.e.*, it will not be obvious that the image has been altered).

Anonymization with passwords. Let $f : \Phi \rightarrow \Gamma$ denote the function mapping face images to people's identities. We would like to condition anonymization via a password p :

$$f(T_p I) \neq f(I), \quad \forall p \in P, \forall I \in \Phi. \quad (3)$$

Deanonymization with inverse passwords. We should recover the original identity only when the correct password is provided. Specifically, the transformer should recover the original face only when the input password is the additive inverse of the password used for anonymization:

$$f(T_{-p} T_p I) = f(T_p^{-1} T_p I) = f(I), \quad \forall p \in P, \forall I \in \Phi, \quad (4)$$

i.e., we model $T_{-p} = T_p^{-1}$.

Wrong deanonymization with wrong inverse passwords. We would like the transformer to change the anonymized identity into a *different* identity that is different from both the original as well as the anonymized image when given a wrong inverse password:

$$f(T_{p'} T_p I) \neq f(I), \quad \forall p, p' \in P, p' \neq -p, \forall I \in \Phi, \quad (5)$$

$$f(T_{p'} T_p I) \neq f(T_p I), \quad \forall p, p' \in P, p' \neq -p, \forall I \in \Phi. \quad (6)$$

In this way, whether the password is correct or not, the identity is always changed so as to confuse the hacker.

Diversity. The transformer should transform I to different identities with different passwords, to increase security in the deanonymization stage (otherwise, if multiple passwords all produce the same identity, a hacker could easily realize that his/her attempts have failed):

$$f(T_{p_1} I) \neq f(T_{p_2} I), \quad \forall p_1, p_2 \in P, p_1 \neq p_2, \forall I \in \Phi. \quad (7)$$

Fig. 2 summarizes our desiderata for anonymization and deanonymization.

4. Approach: Face Identity Transformer

Our face identity transformer T is a conditional GAN trained with a multi-task learning objective. It is conditioned on both the input image I and an input password p . Importantly, the function of p is different from the usual random noise vector z in GANs: z simply tries to model the distribution of the input data, while p in our case makes the

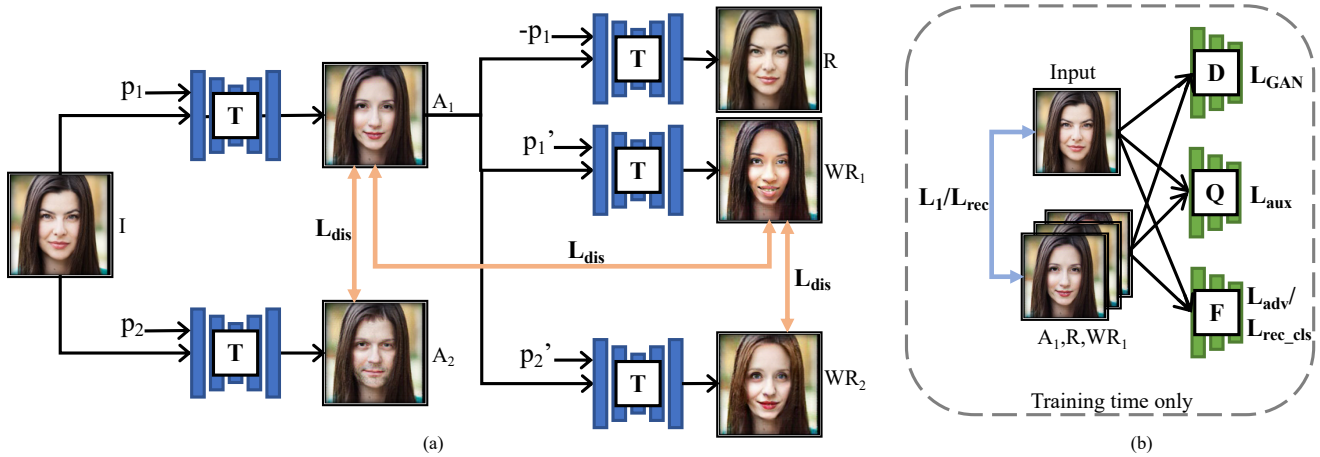


Figure 3: (a) Face identity transformer network architecture. (b) Objectives we apply to synthesized images during training (not included in (a) for clarity). I : Input image, $A_{1,2}$: Anonymized faces, R : Recovered face, $WR_{1,2}$: Wrongly Recovered faces.

transformer hold the desired privacy-preserving properties (Eq. 3-7).

We next explain our password scheme, multimodal identity generation, and multi-task learning objective.

4.1. Password scheme

We use an N -bit string $p \in \{0, 1\}^N$ as our password format, which enables 2^N unique passwords. Given image $I \in \mathbb{R}^{H \times W \times 3}$, we form the input to the transformer as a depthwise concatenation $(I, p) \in \mathbb{R}^{H \times W \times (3+N)}$, where p is replicated in every pixel location. Following InfoGAN [7], we design an auxiliary network $Q(I, T_p I) = \hat{p}$ to predict the embedded password from the input and transformed image pair; *i.e.*, we maximize the mutual information between the identity change in the face image domain and in the password space. We use cross entropy loss for the classifier Q , and denote it as $\mathcal{L}_{aux}(T, Q)$.

4.2. Multimodal identity change

Conditional GANs with random noise do not produce highly stochastic output [17, 12]. To overcome this, BicycleGAN [37] uses an explicitly-encoded multimodality strategy similar to our auxiliary network Q . However, even with Q , we only observe multimodality on colors and textures as in [37], but not on high-level face identity.

Thus, to induce diverse high-level identity changes, we incorporate an explicit feature dissimilarity loss. Specifically, we use a face recognition model F to extract deep embeddings of the faces, and minimize their cosine similarity when they are associated with different passwords:

$$\mathcal{L}_{dis}(M_1, M_2) = \max(0, \cos(F_{embed}(M_1), F_{embed}(M_2))),$$

where \cos is cosine similarity, and M_1 and M_2 are two

transformed face images with two different passwords. We do not penalize pairs whose two features have an angle larger than 90° on the hypersphere; *i.e.*, it is enough for the faces to be different only up to a certain point.

We apply the dissimilarity loss between (1) two anonymized faces with different passwords, (2) two deanonymized faces given different wrong passwords, and (3) the anonymized face and wrongly recovered face:

$$\begin{aligned} \mathcal{L}_{feat}(T) = & \mathbb{E}_{(I, p_1 \neq p_2)} \mathcal{L}_{dis}(T_{p_1} I, T_{p_2} I) \\ & + \mathbb{E}_{(I, p'_1 \neq p'_2, p'_1 \neq -p, p'_2 \neq -p)} \mathcal{L}_{dis}(T_{p'_1} T_p I, T_{p'_2} T_p I) \\ & + \mathbb{E}_{(I, p' \neq -p)} \mathcal{L}_{dis}(T_p I, T_{p'} T_p I) \end{aligned}$$

This loss can be easily satisfied when the model outputs extremely different content that do not necessarily look like a face, and thus can adversely affect other desideratum (*e.g.*, photo-realism) of a privacy-preserving face identity transformer. We next introduce a multi-task learning objective to balance this loss.

4.3. Multi-task learning objective

We describe our multi-task objective that further aids identity change, identity recovery, and photo-realism.

Face classification adversarial loss. We apply the face classification adversarial loss from [23], which helps change the input face's identity. We apply it on both the transformed face $T_p I$ as well as the reconstructed face with wrong recovery password $T_{p'} T_p I$:

$$\begin{aligned} \mathcal{L}_{adv}(T, F) = & -\mathbb{E}_I \mathcal{L}_{CE}(F(I), y_I) - \mathbb{E}_{(I, p)} \mathcal{L}_{CE}(F(T_p I), y_I) \\ & - \mathbb{E}_{(I, p' \neq -p)} \mathcal{L}_{CE}(F(T_{p'} T_p I), y_I) \end{aligned}$$

where F is the face classifier, y_I is face identity label, and \mathcal{L}_{CE} denotes cross entropy loss.

Method	Anonymize?	Deanonymize?	Password-conditioned?
Ren <i>et al.</i> [23]	✓	✓	✗
Super-pixel	✓	✓	✗
Edge	✓	✓	✗
Blur	✓	✗	✗
Noise	✓	✓	✗
Masked	✓	✗	✗
Ours	✓	✓	✓

Table 1: Privacy-preserving ability comparison. Our method is the only one that supports password-conditioned face (de)anonymization without sacrificing privacy.

Similar to the dissimilarity loss (\mathcal{L}_{dis}), this loss pushes the transformed face to have a different identity. The key difference is that this loss requires face identity labels so cannot be used to push $T_{p_1}I$ and $T_{p_2}I$ to have different identities, but has the advantage of trying to keep the transformed image on the face manifold (since the pre-trained face classifier must operate on it in a meaningful way) to improve face realism.

Reconstruction losses. We use L_1 reconstruction loss:

$$\mathcal{L}_{rec}(T) = \|T_{-p}T_pI - I\|_1.$$

With the L_1 loss alone, we find the reconstruction to be often blurry. Hence, we also put a face classification loss $\mathcal{L}_{rec.cls}$ on the reconstructed face to enforce the transformer to recover the high-frequency identity information:

$$\mathcal{L}_{rec.cls}(T, F) = \mathbb{E}_{(I,p)} \mathcal{L}_{CE}(F(T_{-p}T_pI), y_I).$$

This loss enforces reconstructed face $T_{-p}T_pI$ to be predicted as having the same identity as I by face classifier F .

Background preservation loss. For any transformed face, we try to preserve its original background. To this end, we apply another L_1 loss (with lower weight):

$$\mathcal{L}_1(T) = \|T_pI - I\|_1 + \|T_{p'}T_pI - I\|_1.$$

Although employing a face segmentation algorithm is an option, we find that applying \mathcal{L}_1 on the whole image works well to preserve the background.

Photo-realism loss. We use a photo-realism adversarial loss \mathcal{L}_{GAN} [10] on generated images to help model the distribution of real faces. Specifically, we use PatchGAN [12] to restrict the discriminator D 's attention to the structure in local image patches.

4.4. Full objective

Overall, our full objective is:

$$\begin{aligned} \mathcal{L} = & \lambda_{aux} \mathcal{L}_{aux}(T, Q) + \lambda_{feat} \mathcal{L}_{feat}(T) \\ & + \lambda_{adv} \mathcal{L}_{adv}(T, F) + \lambda_{rec.cls} \mathcal{L}_{rec.cls}(T, F) \\ & + \lambda_{rec} \mathcal{L}_{rec}(T) + \lambda_{L_1} \mathcal{L}_1(T) + \mathcal{L}_{GAN}(T, D). \end{aligned} \quad (8)$$

Method	CASIA				LFW			
	LPIPS	DSSIM	L_1	L_2	LPIPS	DSSIM	L_1	L_2
Blur	0.30	0.21	0.12	0.04	0.34	0.24	0.14	0.05
Masked	0.10	0.09	0.07	0.02	0.16	0.13	0.10	0.05
Noise	0.12	0.12	0.07	0.01	0.13	0.12	0.08	0.01
Superpixel	0.09	0.10	0.06	0.01	0.10	0.11	0.07	0.02
Edge	0.25	0.24	0.25	0.24	0.28	0.26	0.29	0.18
Ren et al	0.08	0.07	0.06	0.009	0.08	0.07	0.06	0.010
Ours	0.03	0.03	0.04	0.004	0.04	0.03	0.04	0.004

Table 2: Reconstruction error on CASIA and LFW. Our approach produces the best deanonymizations.

We optimize the following minimax problem to obtain our face identity transformer:

$$T^* = \arg \min_{T, Q} \max_{D, F} \mathcal{L}$$

Training. Fig. 3 shows our network for training. For each input I , we randomly sample two different passwords for anonymization and two incorrect passwords for wrong recoveries, and then impose \mathcal{L}_{dis} on the generated pairs and enforce \mathcal{L}_{dis} between the anonymization and wrong reconstruction. By symmetry and to save memory, we apply \mathcal{L}_{GAN} , \mathcal{L}_{aux} , \mathcal{L}_{adv} , \mathcal{L}_1 only to the first anonymization and first wrong recovery, which empirically works well.

We adopt a two-stage training strategy for the minimax problem [10]. In the discriminator's stage, we fix the parameters of T , Q , and update D , F ; in the generator's stage, we fix D , F , and update T , Q .

Inference. During testing, the transformer T takes as input a user-defined password and face image, anonymizes the face, and saves it to disk. When the user/hacker wants to see the original image, the transformer takes the recovery password and anonymized image, and either outputs the identity-recovered image or a hacker-fooling image depending on password correctness. Throughout the whole process, the original images and passwords are never saved on disk for privacy reasons.

5. Experiments

We show that our face identity transformer achieves password-conditioned anonymization and deanonymization with photo-realism and multimodality. We also conduct ablation studies to analyze each module/loss.

Implementation details. Our identity transformer T is built upon the network from [36]. We use size 128x128 for both inputs and outputs. We subtract 0.5 from p before inputting it to the transformer to make the password channels have 0 mean. We set $N=16$. We use the pretrained SphereFace [15] as our face recognition network F for both deep embedding extraction in the feature dissimilarity loss and face classification adversarial training. For each stage,

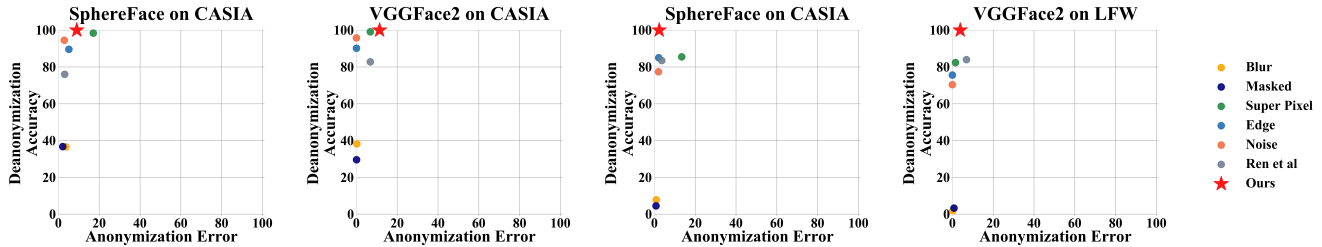


Figure 4: Anonymization vs. deanonimization quality, measured by face verification error/accuracy on CASIA and LFW. Top-left corner is ideal. This result shows that we don’t sacrifice (de)anonymization ability by introducing password conditioning.

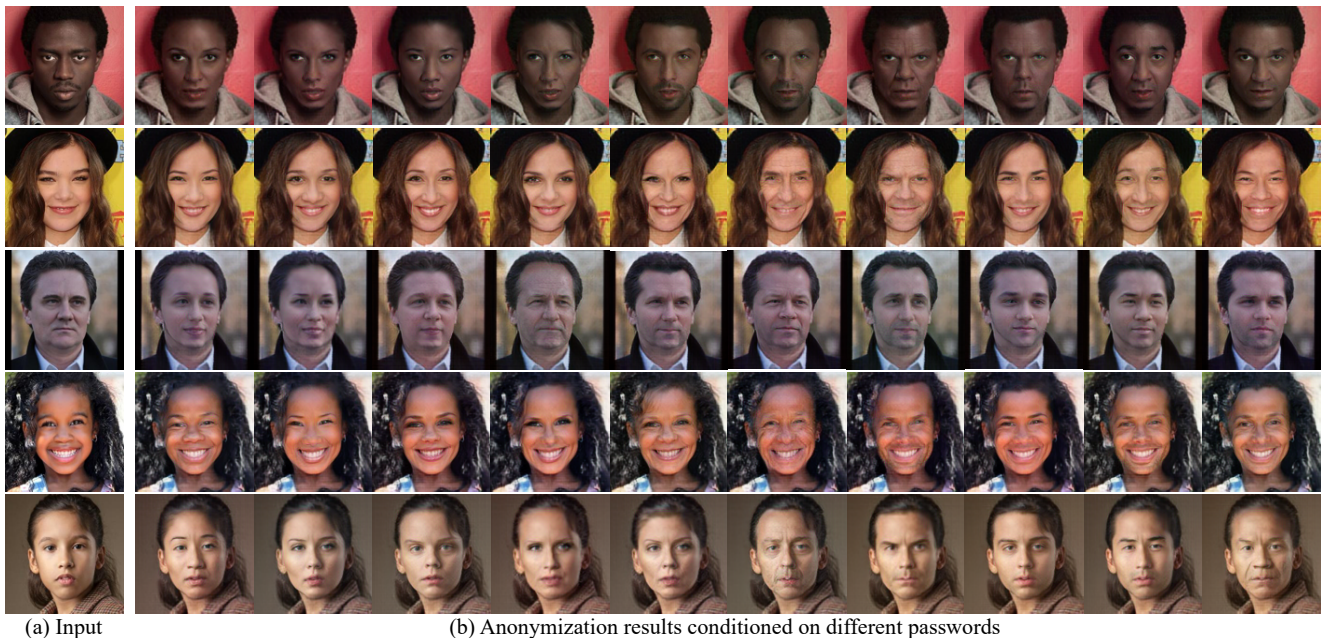


Figure 5: Multimodality results on CASIA. We observe a wide range of identity changes with different passwords.

we use 2 PatchGAN discriminators [12] that have identical structures but operate at different image scales to improve photo-realism. The coarser discriminator is shared among all stages, while three separate finer ones are used for anonymization, reconstruction, and wrong recovery. To improve stability, we use LSGAN [16] and a buffer of 500 generated images when updating D . We set $\lambda_{aux}=1$, $\lambda_{feat}=2$, $\lambda_{adv}=2$, $\lambda_{rec.cls}=1$, $\lambda_{L_1}=10$ and $\lambda_{rec}=100$.

Datasets. 1) CASIA [31] has 454,590 face images belonging to 10,574 identities. We split the dataset into training/validation/testing subsets made up of 80%/10%/10% identities. We use the validation set to select our model. All reported results are on the test set. 2) LFW [11] has 13,233 face images belonging to 5,749 identities. As our network is never trained on LFW, we evaluate on the entire LFW to test its generalization ability. 3) FFHQ [13] is a high-quality face dataset for benchmarking GANs. It is not a face recognition dataset, so we use it for generalization testing only.

We directly test our model on its validation set at 128x128 resolution which contains 10,000 images.

Evaluation metrics. *Face verification accuracy:* We measure our transformer’s identity changing ability with a standard binary face verification test, which scores whether a pair of images have the same identity or not. Since different face recognition models may have different biases, we use two popular pretrained face recognition models: SphereFace [15] and VGGFace2 [4].

Face recovery quality: We measure face recovery quality using **LPIPS distance** [35], which measures perceptual similarity between two images based on deep features, and **DSSIM** [29], which is a commonly-used low-level perceptual metric. We also use pixel-level L_1 and L_2 distance.

AMT perceptual studies: We use Amazon Mechanical Turk (AMT) to test how well our method 1) changes and recovers identities, 2) achieves photo-realism, and 3) attains multimodal anonymizations as judged by human raters.

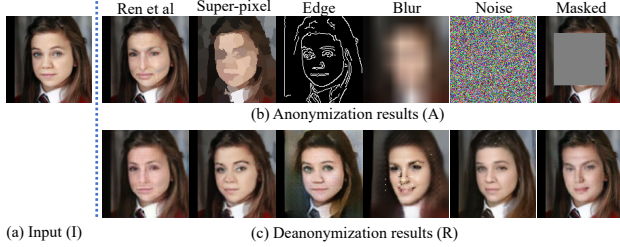


Figure 6: Baselines. Super-pixel, Edge, Blur, Noise, Masked sacrifice photo-realism for anonymization.

5.1. Anonymization and deanonymization

To our knowledge, *no prior work achieves password-conditioned anonymization and deanonymization on visual data like ours*; see Table 1. Hence, we cannot directly compare with any existing method on generating *multimodal* anonymizations and deanonymizations.

Despite this, we want to ensure that our method does no worse than existing methods in terms of anonymization and deanonymization (setting aside the password conditioning capability). To demonstrate this, following [23], we compare to the following baselines: **Ren et al.** [23]: a learned face anonymizer that maintains action detection accuracy; **Superpixel** [3]: each pixel’s RGB value is replaced with its superpixel’s mean RGB value; **Edge** [3]: face regions are replaced with corresponding edge maps; **Blur** [26]: images are downsampled to extreme low-resolution (8×8) and then upsampled back; **Noise**: strong Gaussian noise ($\sigma^2 = 0.5$) is added to the image; **Masked**: face areas ($0.6 \times$ of the face image) are masked out.

We also train deanonymizers for each baseline (*i.e.*, to recover the original face), by using the same generator architecture with our reconstruction and photo-realism losses. Fig. 6 shows a qualitative example of the baselines and their anonymizations/deanonymizations.

Fig. 4 shows anonymization vs. deanonymization (recovery) quality on CASIA and LFW using SphereFace and VGGFace2 as our face recognizers. Our approach performs competitively to Ren et al. [23], “Superpixel”, “Edge”, “Noise”, “Blur”, and “Masked” when considering both anonymization and deanonymization quality together. This result confirms that we do not sacrifice the ability to anonymize/deanonymize by introducing password-conditioning. In fact, in terms of reconstruction (deanonymization) quality (Table 2), our method outperforms the baselines by a large margin because we train our identity transformer to do anonymization and deanonymization in conjunction in an end-to-end way.

Lastly, we perform AMT perceptual studies to rate our anonymizations and deanonymizations. Specifically, we randomly sample 150 testing images (I), and generate for each image: an anonymized face with a random password

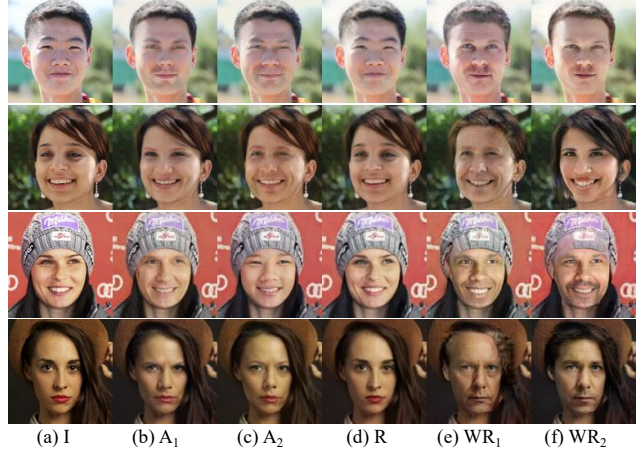


Figure 7: Generalization results on FFHQ. I : original image, $A_{1,2}$: anonymized faces conditioned on different passwords, $R/WR_{1,2}$: recovered faces with correct/wrong passwords.

(A), a recovered face with correct inverse password (R), and a recovered face with wrong password (WR). We then distribute 600 I vs A , I vs R , I vs WR , and A vs WR pairs to turkers and ask “Are they the same person?”. For each pair, we collect responses from 3 different turkers and take the majority as the answer to reduce noise.

The turkers reported 4.7%/100%/0.7%/1.3% on I vs A / I vs R / I vs WR / A vs WR . (low, high, low, low is ideal.) This further shows our method obtains the desired password-conditioned anonymization/deanonymization goals.

5.2. Photo-realism

To evaluate whether our (de)anonymization affects photo-realism, we conduct AMT user studies. We follow the same perceptual study protocol from [36] and test on both anonymizations and wrong recoveries. For each test, we randomly generate 100 “real vs. fake” pairs. For each pair, we average responses from 10 unique turkers. Turkers label our anonymizations as being more real than a real face 30.10% of the time, and label our wrong reconstructions as more real than a real face 15.60% of the time. This shows that our generated images are quite photo-realistic.

5.3. Multimodality

We next evaluate our model’s ability to create different faces given different passwords. Fig. 5 shows qualitative results. Our transformer successfully changes the identity into a broad spectrum of different identities, from women to men, from young to old, *etc.*

We quantitatively evaluate multimodality through an AMT perceptual study. We ask AMT workers to com-



Figure 8: Generalization results on LFW.



Figure 9: Hard cases on CASIA.

pare 150 A_1 vs A_2 and 150 WR_1 vs WR_2 pairs (pairs of anonymized / wrong-recovered faces with different passwords generated from the same input image) and ask “are they the same person?”. The turkers reported “yes” only 12.2% and 2.7% of the time, respectively (lower is better). The results show that our transformer does quite well in changing the identity given different passwords.

5.4. Generalization and difficult cases

Fig. 7 and Fig. 8 show generalization results on FFHQ and LFW using our model trained on CASIA. Without any fine-tuning, our model achieves good generalization performance on both the high quality FFHQ dataset and the LFW dataset where resolution is usually lower. Fig. 9 shows hard-case qualitative results on CASIA. Our method works well even if the faces are with occlusions (sunglasses), with extreme poses, vague, under dim light, etc.

Avg spatial coordinate difference	CASIA	LFW	FFHQ
Bounding boxes	1.81	1.62	1.91
Keypoints	0.94	0.76	0.89

Table 3: Average difference in detected spatial coordinates of face bounding boxes (top-left, bottom-right corners) and 5 keypoints between transformed faces (A , R , WR) and input face (I).

5.5. Applying CV algorithms on transformed faces

Unlike most traditional anonymization algorithms [3, 26], our choice of achieving photo-realism on the (de)anonymizations makes it possible to apply existing computer vision algorithms directly on the transformed faces. To demonstrate this, we apply an off-the-shelf MTCNN [34] face box and keypoint detector on the transformed faces. Qualitative detection results are good. Quantitatively, although we do not have the ground truth annotations for transformed faces, our (de)anonymizations do not change the head/keypoints’ positions from the input faces so we can compare the detection results between the input faces and the transformed faces. Results are shown in Table 3, which shows that a face detection algorithm developed on real images performs accurately on our transformed faces.

5.6. Ablation studies

Finally, we evaluate the contribution of each component and loss in our model. Here, original image (I), anonymized face with two different passwords ($A_{1,2}$), recovered face with correct inverse password (R), and recovered faces with wrong passwords ($WR_{1,2}$):

w/o \mathcal{L}_{dis} : We remove the feature dissimilarity loss on (A_1, A_2) and (WR_1, WR_2) pairs.

w/o WR : We do not explicitly train to produce wrong reconstructions with wrong recovery passwords.

w/o \mathcal{L}_{aux} : We remove the password-predicting auxiliary network Q , but still embed the passwords.

w/o $\mathcal{L}_{rec.cls}$: We remove the face classification loss ($\mathcal{L}_{rec.cls}$) on the reconstruction.

Fig. 10 shows the typical drawbacks of each ablation model. $w/o \mathcal{L}_{dis}$ shows that \mathcal{L}_{dis} is necessary to achieve semantic-level multimodality on both anonymization and wrong reconstruction. $w/o WR$ shows that without training for wrong reconstructions, the transformer fails to conceal identities when given incorrect passwords. $w/o \mathcal{L}_{aux}$ verifies the importance of the auxiliary network, which helps improve photo-realism and we also observe it helps with multimodality. Without $\mathcal{L}_{rec.cls}$, the reconstruction quality suffers because of unbalanced losses.



Figure 10: Typical failure examples of each ablation.

6. Discussion

We feel that this paper has shown the promise of password-conditioned face anonymization and deanonymization to address the privacy versus accessibility tradeoff. That said, our method is not without limitations. We notice artifacts in some generated images, which is more common for wrong reconstructions since the input image goes through the transformer twice. Although improving the quality of the generated images is not our major focus, this problem could potentially be mitigated with a larger training batch size and more stability in optimization. We leave this for future work.

Acknowledgements

This work was supported in part by NSF IIS-1812850, NSF IIS-1812943, NSF CAREER IIS-1751206, AWS ML Research Award, and Google Cloud Platform research credits.

References

- [1] Martin Abadi, Andy Chu, Ian Goodfellow, H Brendan McMahan, Ilya Mironov, Kunal Talwar, and Li Zhang. Deep learning with differential privacy. In *CCS*, 2016. 2
- [2] Jianmin Bao, Dong Chen, Fang Wen, Houqiang Li, and Gang Hua. Towards open-set identity preserving face synthesis. In *CVPR*, 2018. 2
- [3] Daniel J Butler, Justin Huang, Franziska Roesner, and Maya Cakmak. The privacy-utility tradeoff for remotely teleoperated robots. In *ICHRI*, 2015. 1, 7, 8
- [4] Qiong Cao, Li Shen, Weidi Xie, Omkar M Parkhi, and Andrew Zisserman. Vggface2: A dataset for recognising faces across pose and age. In *FG*, 2018. 6
- [5] Yue Cao, Bin Liu, Mingsheng Long, and Jianmin Wang. Hashgan: Deep learning to hash with pair conditional wasserstein gan. In *CVPR*, 2018. 2
- [6] Jiawei Chen, Jonathan Wu, Janusz Konrad, and Prakash Ishwar. Semi-coupled two-stream fusion convnets for action recognition at extremely low resolutions. In *WACV*, 2017. 2
- [7] Xi Chen, Yan Duan, Rein Houthoofd, John Schulman, Ilya Sutskever, and Pieter Abbeel. Infogan: Interpretable representation learning by information maximizing generative adversarial nets. In *NeurIPS*, 2016. 2, 4
- [8] Zekeriya Erkin, Martin Franz, Jorge Guajardo, Stefan Katzenbeisser, Inald Lagendijk, and Tomas Toft. Privacy-preserving face recognition. In *PETS*, 2009. 2
- [9] Ran Gilad-Bachrach, Nathan Dowlin, Kim Laine, Kristin Lauter, Michael Naehrig, and John Wernsing. Cryptonets: Applying neural networks to encrypted data with high throughput and accuracy. In *ICML*, 2016. 2
- [10] Ian Goodfellow, Jean Pouget-Abadie, Mehdi Mirza, Bing Xu, David Warde-Farley, Sherjil Ozair, Aaron Courville, and Yoshua Bengio. Generative adversarial nets. In *NeurIPS*, 2014. 5
- [11] Gary B Huang, Marwan Mattar, Tamara Berg, and Eric Learned-Miller. Labeled faces in the wild: A database for studying face recognition in unconstrained environments. In *Workshop on faces in 'Real-Life' Images*, 2008. 2, 6
- [12] Phillip Isola, Jun-Yan Zhu, Tinghui Zhou, and Alexei A Efros. Image-to-image translation with conditional adversarial networks. In *CVPR*, 2017. 2, 4, 5, 6
- [13] Tero Karras, Samuli Laine, and Timo Aila. A style-based generator architecture for generative adversarial networks. *arXiv:1812.04948*, 2018. 2, 6
- [14] Anders Boesen Lindbo Larsen, Søren Kaae Sønderby, Hugo Larochelle, and Ole Winther. Autoencoding beyond pixels using a learned similarity metric. *arXiv:1512.09300*, 2015. 2
- [15] Weiyang Liu, Yandong Wen, Zhiding Yu, Ming Li, Bhiksha Raj, and Le Song. Sphreface: Deep hypersphere embedding for face recognition. In *CVPR*, 2017. 5, 6
- [16] Xudong Mao, Qing Li, Haoran Xie, Raymond YK Lau, Zhen Wang, and Stephen Paul Smolley. Least squares generative adversarial networks. In *ICCV*, 2017. 6
- [17] Michael Mathieu, Camille Couprie, and Yann LeCun. Deep multi-scale video prediction beyond mean square error. *arXiv:1511.05440*, 2015. 4
- [18] Mehdi Mirza and Simon Osindero. Conditional generative adversarial nets. *arXiv:1411.1784*, 2014. 2
- [19] Guim Perarnau, Joost Van De Weijer, Bogdan Raducanu, and Jose M Álvarez. Invertible conditional gans for image editing. *arXiv:1611.06355*, 2016. 2
- [20] Albert Pumarola, Antonio Agudo, Aleix M Martinez, Alberto Sanfeliu, and Francesc Moreno-Noguer. Ganimation: Anatomically-aware facial animation from a single image. In *ECCV*, 2018. 2
- [21] Scott Reed, Zeynep Akata, Xinchun Yan, Lajanugen Logeswaran, Bernt Schiele, and Honglak Lee. Generative adversarial text to image synthesis. *arXiv:1605.05396*, 2016. 2

- [22] Krishna Regmi and Ali Borji. Cross-view image synthesis using conditional gans. In *CVPR*, 2018. 2
- [23] Zhongzheng Ren, Yong Jae Lee, and Michael S Ryoo. Learning to anonymize faces for privacy preserving action detection. In *ECCV*, 2018. 1, 2, 4, 5, 7
- [24] Ronald L Rivest, Adi Shamir, and Leonard Adleman. A method for obtaining digital signatures and public-key cryptosystems. *Communications of the ACM*, 1978. 2
- [25] Michael S Ryoo, Kiyoon Kim, and Hyun Jong Yang. Extreme low resolution activity recognition with multi-siamese embedding learning. In *AAAI*, 2018. 2
- [26] Michael S Ryoo, Brandon Rothrock, Charles Fleming, and Hyun Jong Yang. Privacy-preserving human activity recognition from extreme low resolution. In *AAAI*, 2017. 1, 2, 7, 8
- [27] Wei Shen and Rujie Liu. Learning residual images for face attribute manipulation. In *CVPR*, 2017. 2
- [28] Ting-Chun Wang, Ming-Yu Liu, Jun-Yan Zhu, Andrew Tao, Jan Kautz, and Bryan Catanzaro. High-resolution image synthesis and semantic manipulation with conditional gans. In *CVPR*, 2018. 2
- [29] Zhou Wang, Alan C Bovik, Hamid R Sheikh, Eero P Simoncelli, et al. Image quality assessment: from error visibility to structural similarity. *IEEE TIP*, 13(4):600–612, 2004. 6
- [30] Zhangyang Wang, Shiyu Chang, Yingzhen Yang, Ding Liu, and Thomas S Huang. Studying very low resolution recognition using deep networks. In *CVPR*, 2016. 2
- [31] Dong Yi, Zhen Lei, Shengcai Liao, and Stan Z Li. Learning face representation from scratch. *arXiv:1411.7923*, 2014. 2, 6
- [32] Ryo Yonetani, Vishnu Naresh Boddeti, Kris M Kitani, and Yoichi Sato. Privacy-preserving visual learning using doubly permuted homomorphic encryption. In *ICCV*, 2017. 2
- [33] Han Zhang, Tao Xu, Hongsheng Li, Shaoting Zhang, Xiaogang Wang, Xiaolei Huang, and Dimitris N Metaxas. Stackgan: Text to photo-realistic image synthesis with stacked generative adversarial networks. In *ICCV*, 2017. 2
- [34] Kaipeng Zhang, Zhanpeng Zhang, Zhifeng Li, and Yu Qiao. Joint face detection and alignment using multitask cascaded convolutional networks. *IEEE Signal Processing Letters*, 23(10):1499–1503, 2016. 8
- [35] Richard Zhang, Phillip Isola, Alexei A Efros, Eli Shechtman, and Oliver Wang. The unreasonable effectiveness of deep features as a perceptual metric. In *CVPR*, 2018. 6
- [36] Jun-Yan Zhu, Taesung Park, Phillip Isola, and Alexei A Efros. Unpaired image-to-image translation using cycle-consistent adversarial networks. In *ICCV*, 2017. 5, 7
- [37] Jun-Yan Zhu, Richard Zhang, Deepak Pathak, Trevor Darrell, Alexei A Efros, Oliver Wang, and Eli Shechtman. Toward multimodal image-to-image translation. In *NeurIPS*, 2017. 4
- [38] Shizhan Zhu, Raquel Urtasun, Sanja Fidler, Dahua Lin, and Chen Change Loy. Be your own prada: Fashion synthesis with structural coherence. In *ICCV*, 2017. 2